

# The subarctic frontal zone in the North Pacific: Characteristics of frontal structure from climatological data and synoptic surveys

Xiaojun Yuan

Lamont-Doherty Earth Observatory, Palisades, New York

Lynne D. Talley

Scripps Institution of Oceanography, La Jolla, California

**Abstract.** The subarctic front is a thermohaline structure across the North Pacific, separating colder, fresher water to the north from warmer, saltier water to the south. Levitus's [1982] data and 72 conductivity-temperature-depth/salinity-temperature-depth sections are used to show the spatial and seasonal variations of the climatological frontal zone and the characteristics of the frontal structure in synoptic surveys. The temperature gradient in the mean frontal zone is stronger in the western Pacific and decreases eastward, while the salinity gradient has less variation across the Pacific. The temperature gradient also has larger seasonal variation, with a maximum in spring, than the salinity gradient. The synoptic surveys show that the frontal zone is narrower and individual fronts tend to be stronger in the western Pacific than in the eastern Pacific. Density gradients tend to be more compensated at the strongest salinity fronts than at the strongest temperature fronts. A horizontal minimum of vertical stability is found south of the subarctic halocline outcrop. The northern boundary of the North Pacific Intermediate Water merges with the frontal zone west of 175°W and is north of the northern boundary of the subarctic frontal zone in the eastern Pacific. The shallow salinity minima start within the subarctic frontal zone in the eastern Pacific.

## 1. Introduction

The subarctic frontal zone (SFZ), a permanent thermohaline structure across the North Pacific, has been the subject of many studies [Sverdrup *et al.*, 1942; Dodimead *et al.*, 1963; Uda, 1963; Roden, 1964, 1972, 1975, 1977, 1991; Camerlengo, 1982; Lynn, 1986; Roden and Robinson, 1988; Zhang and Hanawa, 1993; Yoshida, 1993; Kazmin and Rienecker, 1996]. It separates two distinct water masses: colder, fresher water to the north and warmer, saltier water to the south. The SFZ usually contains a couple of temperature and salinity fronts [Roden, 1977]. Those individual fronts are usually sharp and time dependent. The location of the SFZ, however, is rather permanent. No clear seasonal or interannual variations of the SFZ location have been found [Yoshida, 1993], although seasonal variation of the strength of the subarctic temperature front was detected in the western North Pacific [Roden, 1980] and central North Pacific [Kazmin and Rienecker, 1996] by satellite observations. Within the frontal zone, horizontal temperature and salinity gradients in the mixed layer point in the same direction; thus the resulting density gradients are weak [Roden, 1975, 1977, 1984]. A moderate density gradient can be found below the mixed layer in the central North Pacific, associated with the broad eastward flow called "west wind drift."

In synoptic surveys the subarctic frontal zone has shown a variety of structures. In the western North Pacific, quasi-regularly spaced density fronts are found from the surface to a

depth of about 1 km, with associated baroclinic flows of up to  $0.6 \text{ m s}^{-1}$  [Roden, 1984]. However, the density front becomes weak in the mixed layer in the central and eastern North Pacific. Intense temperature and salinity fronts are found in the mixed layer and decay rapidly below. The fronts are much shallower in the central and eastern Pacific than in the western Pacific. The subarctic permanent halocline outcrops in the subarctic frontal zone. The outcropping terminates the high stability layer within the permanent pycnocline in the subarctic ocean. A gap in high stability, defined by a horizontal minimum of the vertical maximum of Väisälä frequency, exists south of the subarctic frontal zone [Roden, 1970, 1972]. The stability gap allows the vertical mixing to penetrate to a greater depth south of the frontal zone, which is related to the formation of the North Pacific Central Mode Water (T. Suga *et al.*, Thermocline distribution in the North Pacific subtropical gyre: The Subtropical Mode Water and the Central Mode Water, submitted to *Journal of Physical Oceanography*, 1996; hereinafter referred to as Suga *et al.*, submitted manuscript, 1996; H. Nakamura, A pycnocline on the bottom of the ventilated portion in the central subtropical North Pacific: Its distribution and formation, submitted to *Journal of Physical Oceanography*, 1996; hereinafter referred to as Nakamura, submitted manuscript, 1996) and may also be related to the subarctic frontogenesis.

Ekman convergence was suggested as a major mechanism for subarctic frontogenesis [Roden, 1970, 1977]. However, the large seasonal variation of wind field (shown in a following paper) and the relatively stable location of the front imply that some other frontogenetic mechanism may exist. For example,

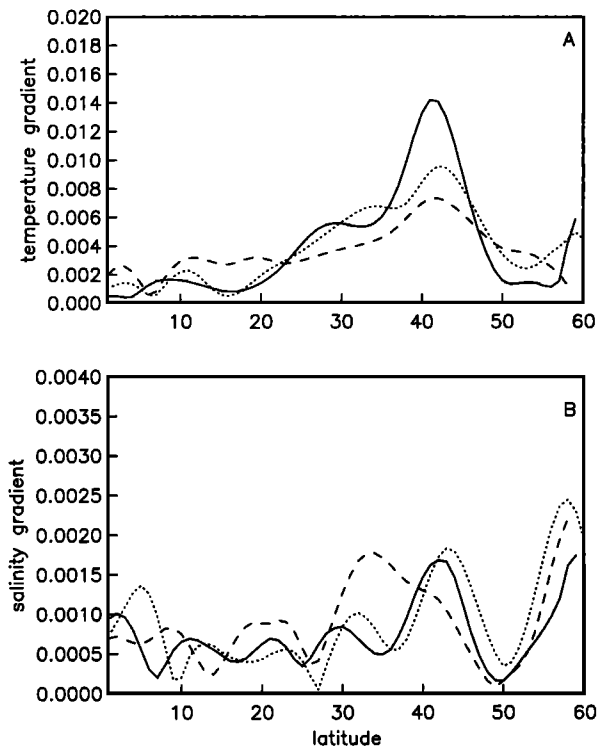


**Figure 1.** Horizontal gradients of Levitus's [1982] annual mean (a) temperature and (b) salinity at 10-m depth along meridians of 165°E (solid lines), 170°W (dotted lines), and 140°W (dashed lines), which represent the western, central, and eastern North Pacific, respectively. Units of temperature gradients are degrees Celsius per kilometer. Units of salinity gradient are parts per thousand per kilometer.

the subarctic front may originate from the Oyashio front in the western North Pacific and be advected across the Pacific by the general circulation. Weak and sporadic Ekman convergence could then maintain the front.

Previous studies offer information about the subarctic front at certain locations and certain seasons. In this study we examine the temporal and spatial variabilities of the strength and location of the subarctic front across the North Pacific using both climatological data and synoptic surveys. Quantifying the density compensating nature of the front and investigating the distribution of the stability gap south of the front are the goals of this study. Other characteristics of the front, such as typical frontal zone structure and mixed layer depth across the front, are also addressed.

This paper consists of two parts. The first part concentrates on the climatological frontal zone using Levitus's [1982] temperature and salinity data. The detailed frontal structure and its main characteristics are then studied using 72 cross-front conductivity-temperature-depth/salinity-temperature-depth (CTD/STD) sections in the second part of the paper. Underway data along 135°W provide an example of the actual width of an individual front. The frontal structure and characteristics in synoptic observations are compared with the climatological frontal zone. Some possible mechanisms for frontogenesis are also discussed.

## 2. Climatological Subarctic Frontal Zone

Levitus's [1982] gridded data are based on all available oceanographic data existing before 1978, including oceanographic

station data, expendable bathythermograph (XBT) data, mechanical bathythermograph (MBT) data, and CTD/STD data. Careful quality control and then objective analysis were applied to the data. The resulting climatological seasonal and annual mean temperature and salinity are on a  $1^\circ \times 1^\circ$  grid. The temperature and salinity fields are heavily smoothed in his analysis scheme. The amplitude of his response function is close to zero near a wavelength of 500 km, so that any variation with length scale less than 500 km is smoothed out. The frontal signals left in the Levitus's data represent mean and smoothed conditions. Since frontal scales in a real ocean are usually much smaller than Levitus's smoothing scale and frontal location moves with time, the mean frontal structure can be very different from a single synoptic survey. We define the subarctic temperature and salinity fronts in Levitus's [1982] data by the maximum of horizontal temperature and salinity gradients, respectively. This definition will not be applied to synoptic surveys. In this paper the subarctic front refers to the subarctic frontal zone, and the subtropical front means the subtropical frontal zone.

### 2.1. The Mean Temperature and Salinity Fronts

Levitus's [1982] annual mean temperature and salinity at 10-m depth are used to investigate the climatological subarctic frontal zone in the North Pacific upper ocean. Horizontal gradients of temperature and salinity at 10-m depth are calculated. The magnitude of horizontal temperature and salinity gradients is defined as

$$G_T = |\nabla_H T| = \sqrt{(\partial T/\partial x)^2 + (\partial T/\partial y)^2} \quad (1)$$

$$G_S = |\nabla_H S| = \sqrt{(\partial S/\partial x)^2 + (\partial S/\partial y)^2}. \quad (2)$$

Horizontal temperature and salinity gradients in the western, central, and eastern North Pacific are plotted in Figure 1. Despite heavy horizontal smoothing in the data and averaging over four seasons, high horizontal gradients in the subarctic frontal zone between 40°N and 44°N stand out significantly. The strongest annual mean subarctic temperature front is found in the western North Pacific, and the weakest front occurs in the eastern North Pacific. The subtropical frontal zone, which is near 30°N [Roden, 1980], is very weak in the western and central Pacific and absent in the eastern Pacific in the annual mean temperature data. The strength of the subarctic salinity front has less variation across the Pacific than the temperature front. The salinity front in the central Pacific is slightly north of the salinity front in the western Pacific and is slightly stronger. The subarctic salinity front in the eastern North Pacific is the broad high gradient region centered at 33°N; Lynn [1986] reported that the subarctic front turns southward and becomes closer to the subtropical front in the eastern North Pacific. The broadness of the high gradient regions results from smoothing over the subarctic and subtropical fronts in Levitus's [1982] data processing. The subtropical salinity front in the western and central North Pacific is weaker than and clearly separated from the subarctic front.

The frontal positions can be identified by the clear maxima of the gradients (Figure 1). Locations of maximum temperature and salinity gradients are selected throughout the North Pacific at the depths of 10 and 100 m (Figure 2). The subarctic front, subtropical front, and doldrum front can be identified in both temperature and salinity fields. However, the Kuroshio front which occurs between 30° and 40°N in the western Pacific [Mizuno and White, 1983] surprisingly is missing at both depths.

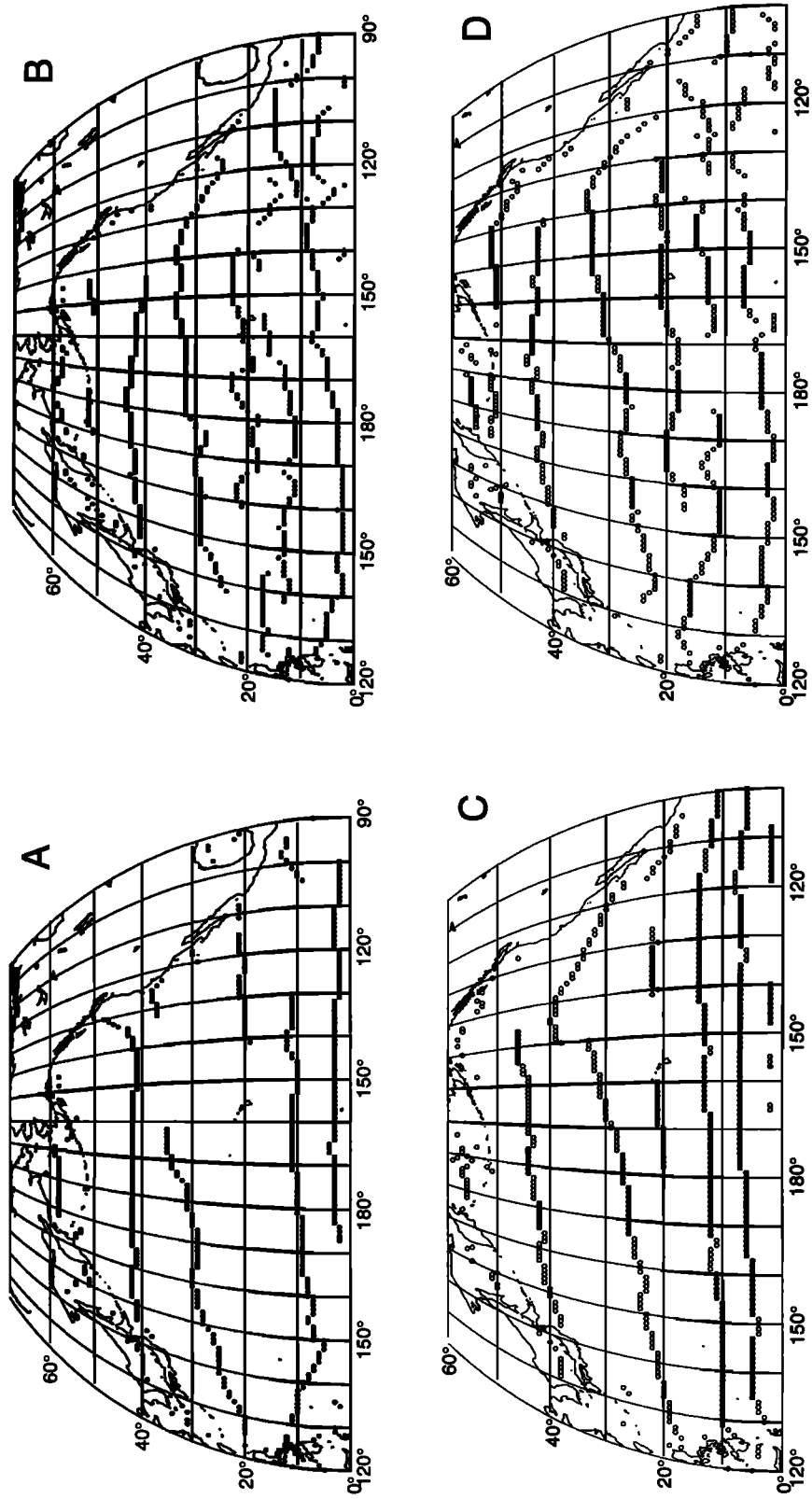
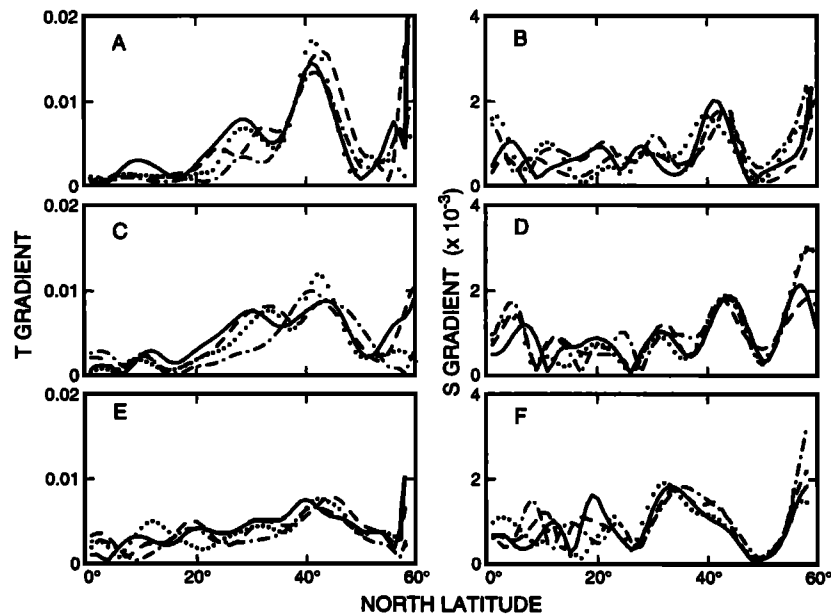


Figure 2. (a) Temperature fronts and (b) salinity fronts at a depth of 10 m and (c) temperature gradients by the maxima of horizontal gradients from *Levitus's* [1982] annual mean data. at a depth of 100 m in the North Pacific identified by the maxima of horizontal gradients from *Levitus's* [1982] annual mean data.



**Figure 3.** Horizontal temperature and salinity gradients (a–b) along 165°E, (c–d) along 170°W, and (e–f) along 140°E from *Levitus's* [1982] winter (solid lines), spring (dotted lines), summer (dashed-dotted lines), and fall (dashed lines) data at a depth of 10 m. Units are degrees Celsius per kilometer and parts per thousand per kilometer for temperature and salinity, respectively.

The subtropical temperature front is also missing at the 10-m depth in the eastern Pacific.

At the depth of 10 m the subarctic temperature front starts from the coast of Japan and crosses the North Pacific between 41°N and 42°N. When it reaches 140°W, the front splits into two parts: one turns northeast, and the other shifts southward. The subtropical temperature front starts from 20°N in the western Pacific and extends northeastward. This front loses its identity east of 160°W. Two large-scale temperature fronts are found across the Pacific in the equatorial region. These two fronts coincide with the northern and southern doldrum fronts, although *Roden* [1974, 1975] suggested that they are only clearly recognized as salinity and density fronts.

The subarctic salinity front crosses the Pacific between 40° and 44°N in the mixed layer. Its position is slightly different from the temperature front. East of 140°W, the subarctic salinity front turns southward with the California Current and merges with the subtropical front due to the smoothing in the data. South of 20°N, the salinity fronts become noisy. The doldrum front is identifiable but not in the same location as *Roden* [1974, 1975] suggested.

Below the seasonal thermocline, which is usually at a depth of 30 m in the midlatitudes of the North Pacific, the subarctic temperature front shifts a few degrees of latitude to the north, while the subtropical temperature front shifts several degrees to the south in the central North Pacific (Figure 2c). A clear temperature front appears at 100-m depth in the eastern Pacific, which may result from the smoothing over the subarctic and subtropical fronts. The vertical displacement of the subarctic temperature front is mainly due to the seasonal variation of the front in the mixed layer. In summer the front at 10-m depth is a few degrees of latitude south of the front at 100-m depth, which occurs at the same location of the winter surface front, in most areas of the North Pacific except in the western and eastern boundary regions (not shown here). The subarctic salinity front has the similar vertical structure.

## 2.2. Annual Variation of the Subarctic and Subtropical Fronts

*Levitus's* [1982] seasonal mean data are used to show the seasonal variations of the subarctic front. Temperature and salinity gradients at 10-m depth are defined as in (1) and (2). In the western North Pacific (165°E), intensity of the subarctic temperature front (defined by the magnitude of the maximum temperature gradient) undergoes a seasonal cycle (Figure 3a). The strongest front occurs in spring with a magnitude of 0.017°C/km, and the weakest front is found in summer. The intensity of the front is 27% stronger in spring than in summer at this longitude. This implies that unevenly distributed surface heating in spring is important in frontogenesis. The location of the subarctic temperature front apparently moves only about 2 degrees latitude annually. The position of the subtropical thermal front has a larger annual variation than the subarctic front. The resulting annual mean surface temperature gradient at the subtropical front is small (Figure 1). The subarctic salinity front has an annual variation of 23% in its intensity. The front moves 3 degrees annually from 40° to 43°N in the western North Pacific (Figure 3b).

In the central North Pacific (170°W), apparent annual motion of the subarctic temperature front is 3 degrees of latitude, from 41°N to 44°N (Figure 3c). It has a 39% annual variation in its intensity. The front is strongest in spring with a magnitude of 0.012°C/km. This frontal strength is comparable to *Kazmin and Rienecker's* [1996] zonally averaged 10-year mean gradients in the central Pacific. The subtropical thermal front has a relatively small variation of intensity in winter, spring, and fall. However, it disappears in summer because of stronger and more uniformly distributed surface heating. The subarctic salinity front has a very small annual variation in both location and intensity in the central North Pacific, as does the subtropical salinity front (Figure 3d).

Figures 3e and 3f show annual variations of temperature and

salinity gradients in the eastern North Pacific. The subarctic temperature front apparently moves 5 degrees annually from 40° to 45°N and has a small annual variation in intensity. A separate subtropical thermal front is still visible, except in summer. The subarctic salinity front in the eastern Pacific is located further south than in the western and central Pacific and is combined with the subtropical salinity front to form a broad frontal region. Again, the merger of the two fronts is largely due to the heavy smoothing applied by *Levitus* [1982]. The location of the maximum salinity gradient of the broad frontal zone moves 4 degrees of latitude. However, the magnitude of the maximum has a small annual variation.

Annual variations of temperature and salinity at the subarctic front are listed in Table 1. The variability of temperature at the temperature front is the strongest in the central Pacific: 10.44°C. The variation of temperature at the front exceeds 7°C in both the eastern and western Pacific. These variations are 5–10 times larger than the maximum temperature change across 100 km in the frontal zone. The salinity at the subarctic salinity front has an annual range of 0.23‰ in both the western and central Pacific. This variation is comparable to the maximum salinity change across 100 km in the frontal zone. In the eastern Pacific the variation is double.

It is worth mentioning that the apparently annual motions of the climatological subarctic temperature and salinity fronts are not the movements of isotherms and isohalines. The maxima temperature and salinity gradients occur at different isotherms and isohalines in different seasons (Table 1). For example, the subarctic temperature appears to migrate to the south during summer in the central Pacific (Figure 3c) and occurs at the isotherm of 16.8°C (comparing to the isotherm of 9.11°C in winter). However, this apparent migration does not tell us if the front is advected southward and warmed up in the same time or a new front is formed in the south due to changes of surface frontogenetic forcing including solar radiation and wind stress. The subarctic front in the mixed layer is more vulnerable to the surface forcing during summer since the seasonal thermocline is at a depth of about 30 m in the mid-latitude North Pacific. However, the front at permanent pycnocline may be more constrained by the general circulation and water mass distribution of the North Pacific. To understand the apparent movement of the front, we need to understand dynamical processes of subarctic frontogenesis in different seasons and at different depths.

### 2.3. Stability Gap in Winter

The subarctic ocean is characterized by a permanent halocline between 100 and 150 m in winter and a seasonal thermocline between 30 and 60 m in summer [Roden, 1977]. The permanent halocline outcrops near the subarctic frontal zone, so that the outcroppings of the isohalines near the top and bottom of the halocline can be used to define the subarctic frontal zone [Roden, 1991]. In winter, vertical mixing destroys the seasonal thermocline, which is formed in both gyres in summer, leaving a permanent thermocline in the subtropical gyre and a permanent halocline in the subpolar gyre. A lateral minimum in the high vertical stability associated with the permanent pycnoclines then appears south of the subarctic front because of absence of the permanent halocline and weak permanent thermocline.

Roden [1970, 1972] termed the lateral minimum in the vertical stability the "stability gap." The gap is thus usually associated with the southern boundary of the subarctic halocline,

**Table 1.** Temperature at the Subarctic Temperature Front and Salinity at the Subarctic Salinity Front in the Western (165°E), Central (170°W), and Eastern (140°W) North Pacific (NP) in *Levitus's* [1982] Data

	Western NP		Central NP		Eastern NP	
	<i>T</i> , °C	<i>S</i> , ‰	<i>T</i> , °C	<i>S</i> , ‰	<i>T</i> , °C	<i>S</i> , ‰
Winter	9.11	33.95	7.79	33.58	12.17	34.40
Spring	13.37	33.91	12.79	33.70	15.32	34.58
Summer	16.80	33.76	18.23	33.47	18.21	34.16
Fall	9.38	33.72	10.18	33.57	11.00	34.42

The subarctic temperature and salinity fronts are defined by the maximum horizontal temperature and salinity gradient, respectively.

which outcrops in the subarctic frontal zone. We use the horizontal minimum of vertical maximum Väisälä frequency, which was also used by Roden [1970, 1972], to identify the stability gap.

Väisälä frequency along 155°W is calculated from *Levitus's* [1982] winter data and plotted along with winter temperature and salinity (Figure 4). A high stability layer near 100 m occurs north of 45°N in the subarctic domain and between 29°N and 38°N in the subtropical gyre. The stability is reduced between 38°N and 45°N. In the subarctic gyre the maximum Väisälä frequency coincides with the halocline. The maximum Väisälä frequency decreases in the region of the halocline outcropping. In the subtropical gyre the high-stability layer coincides with the permanent thermocline.

The winter stability gap can be found in most regions of the North Pacific between the permanent subpolar halocline and the subtropical thermocline, although its width varies spatially. The magnitude of the largest vertical maximum of the Väisälä frequency above 400 m is contoured in Figure 5. A horizontal minimum of vertical Väisälä frequency maximum is found around 40°N in the western and central North Pacific. In the eastern Pacific, another branch of the minimum is found near 30°N. The minima suggest lower stability in these areas. The depth of the maximum Väisälä frequency is between 100 and 150 m in most regions of the North Pacific. However, it is deeper in the less stable areas. The fastest deepening occurs near the boundaries of the these areas. Especially in the southern boundary, a merging of a shallow stable layer south of the less stable areas soars the depth from 300 to 100 m in a very short distance.

Reid [1982] used the saturation ratio of dissolved oxygen to indicate the winter mixed layer depth. He found that the winter mixed layer has a deep trough between the subtropical and subarctic gyres, which coincides with the less stable area in Figure 5. However, our vertical maximum of the Väisälä frequency is deeper than Reid's [1982] mixed layer depth.

The existence of the stability gap may allow vertical mixing to penetrate much deeper south of the subarctic front in winter. The deeper mixing and the absence of permanent pycnocline may generate a difference in the mixed layer depth across the front, as is discussed in section 3.6. This sudden change in mixed layer depth could cause a convergence of Ekman velocity without a convergence of Ekman transport.

### 2.4. Density Compensation in the Subarctic Front

Another characteristic of the subarctic front is its density compensating nature. Large horizontal gradients in tempera-

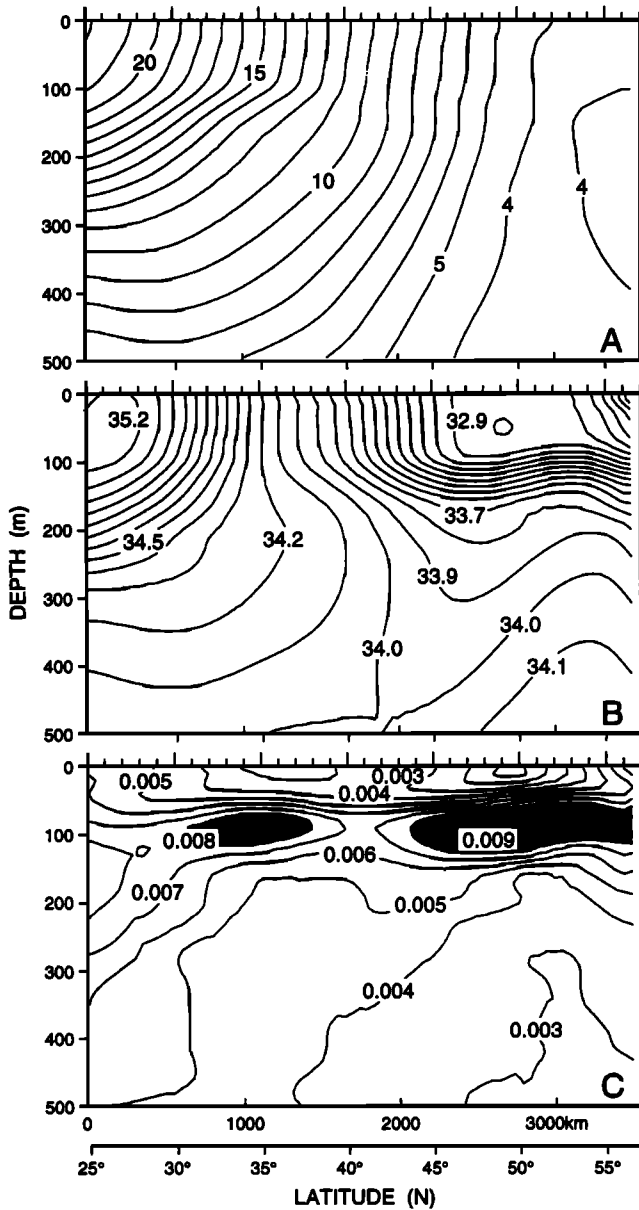


**Figure 4.** (a) Temperature, (b) salinity, and (c) Väisälä frequency along 155°W in winter from *Levitus's* [1982] smoothed data. Väisälä frequencies exceeding 0.08 rad/s are emphasized by shading to show the high stability layer and stability gap centered at 40°–42°N.

ture and salinity in the mixed layer nearly balance each other, and the resulting density gradient is weak. Synoptic surveys from the western to eastern North Pacific [Roden, 1972, 1975, 1977] show the low density gradient in the subarctic frontal zone. The extent of density compensation near the climatological frontal zone should be quantified.

The density ratio, defined by  $R_\rho = \alpha \partial_z T / \beta \partial_z S$  [Turner, 1973], is usually used to show the relative strength of double diffusion. If defined by  $R_\rho = \alpha \partial_y T / \beta \partial_y S$ , it measures the relative importance of horizontal temperature and salinity gradients to the density gradient. However,  $R_\rho$  cannot distinguish among regions where both  $\alpha \partial T$  and  $\beta \partial S$  are positive from those where both are negative. Also, when the salinity gradient becomes very small, the density ratio is singular. *Ruddick*

[1983] introduced the Turner angle to show the strength of double diffusion, avoiding the ambiguity of the density ratio. We adopt *Ruddick's* Turner angle and apply it into horizontal gradients to show the degree of density compensation. Since the meridional gradients of surface temperature and salinity are much greater than the zonal gradients, we neglect the contribution from the latter. Coordinate axes in Turner angle space are defined as  $A_S = \beta \partial_y S$  and  $A_T = \alpha \partial_y T$ , where  $\alpha = \partial \rho / \partial T$  and  $\beta = \partial \rho / \partial S$  (Figure 6).  $Y$  points to the north. Both  $A_S$  and  $A_T$  are positive when density increases northward. The Turner angle is defined by

$$Tu = \arctan [(A_T - A_S) / (A_T + A_S)] \quad (3)$$

following *Ruddick* [1983] and is related to the density ratio by  $R_\rho = -\tan (Tu + 45^\circ)$ . The shaded areas show where the contribution of the salinity gradient to the density gradient exceeds the contribution of the temperature gradient. Complete density compensation occurs at  $Tu = \pm 90^\circ$ , where temperature and salinity gradients have the same direction and  $A_T$  and  $A_S$  have the same magnitude.

Turner angles in the mixed layer in *Levitus's* winter and summer are plotted from 1°N to 65°N in Figure 7. Temperature gradients are stronger than salinity gradients in most of the North Pacific, except in the central and eastern equatorial regions and at high latitudes. As shown in Figure 6, when  $45^\circ < Tu < 90^\circ$ , temperature and salinity both decrease northward, and temperature gradients dominate. This occurs

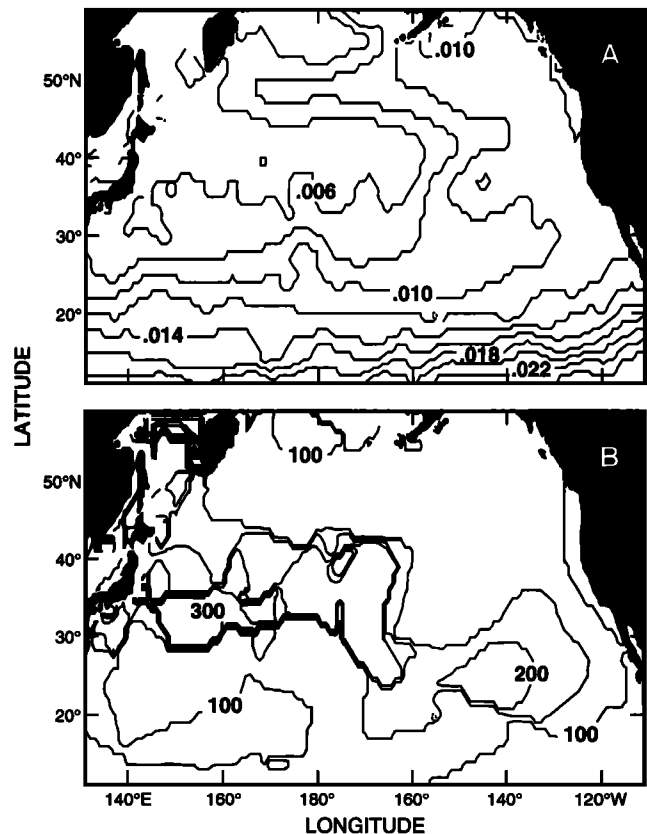


**Figure 5.** (a) Magnitude of the largest vertical maximum of the Väisälä frequency in the upper 400 m in winter from *Levitus's* [1982] data. Units are radians per second. (b) Depth (in meters) of the largest vertical maximum, with a contour interval of 100 m.

between about 25°N and 50°N. We call this region the “temperature-dominated regime.” North of 50°N, Turner angles show that salinity gradients dominate. However, the directions of temperature and salinity gradients change with latitude so the Turner angles are scattered. This region is called the “salinity-dominated regime.” There is a transition area between the temperature-dominated regime and salinity-dominated regime. Density gradients are nearly compensating (Turner angles are close to 90°) in the transition zone. In winter, Turner angles are close to 90° between 42° and 45°N basinwide. The subarctic frontal zone in the western and central Pacific coincides with this area. In the eastern Pacific the subarctic front does not occur in the transition area but further south, where the Turner angles are also close to 90°. In summer, Turner angles are close to 90° in the central Pacific near 45°N and in the eastern Pacific between 33° to 36°N, where the subarctic front is found [Lynn, 1986]. In the western Pacific, less density compensation occurs in the subarctic frontal zone during summer months.

The subarctic front in the western and central Pacific occurs in the transition area, where the ocean changes from the temperature-dominated regime to the salinity-dominated regime. In this transition area, temperature and salinity gradients are roughly compensating so the density gradient is low. Though there are some seasonal and longitudinal variations of the Turner angles in the North Pacific, the general trends are the same in the western and central North Pacific from winter to summer. In the eastern Pacific the frontal zone lies inside the temperature-dominated regime; however, the density at the front still tends to be compensated. We will discuss this again in section 3.7 and section 4.

### 3. The Subarctic Front in Synoptic Observations

The subarctic front in synoptic observations, such as CTD sections, differs from the climatological frontal zone. Closely

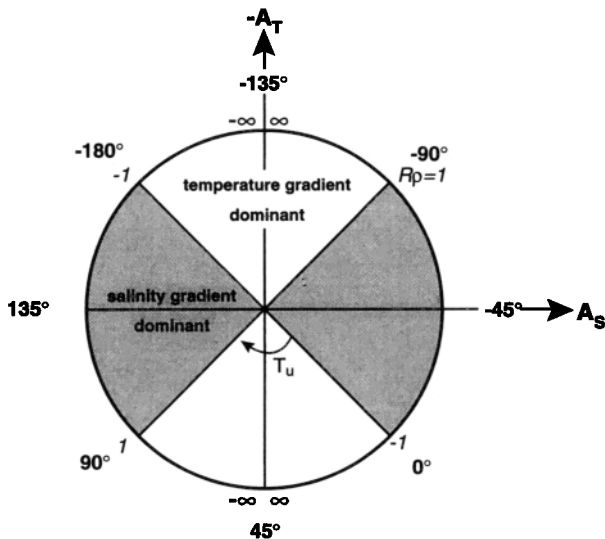


**Figure 6.** The plane  $-A_T = -\alpha\partial_y T$  versus  $A_S = \beta\partial_y S$ . Lines of constant  $R_\rho$  radiate outward at a constant angle from the origin. Some values are shown outside the circle. Increasing Turner angles are in the direction of the arrow. The areas where the salinity gradient contribution to density gradient exceeds temperature’s contribution are shaded. Temperature gradients dominate in unshaded areas.

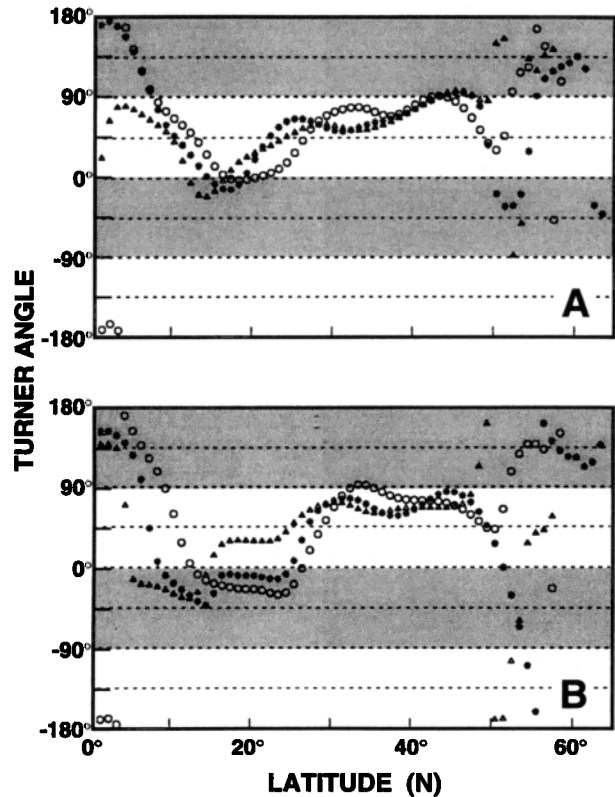


**Figure 7.** Turner angle at 10-m depth from Levitus’s [1982] (a) winter and (b) summer data. Triangles, asterisks, and circles are the Turner angles in the western (165°E), central (175°W), and eastern (140°E) North Pacific, respectively. Shaded areas show where salinity gradients dominate. Temperature gradients dominate in unshaded areas.

spaced CTD/STD data from research vessels give snapshots of the frontal zone, which exhibit a rich variety of detailed structure [Roden, 1972, 1977; Lynn, 1986]. A few sharp individual temperature and salinity fronts can usually be found within the frontal zone. The width, penetration depth, intensity, and location of these fronts vary spatially and temporally. Roden [1984] has shown mesoscale oceanic fronts in the western North Pacific, which are related to large-amplitude density oscillations below the mixed layer. A few three-dimensional observations and satellite data show meandering of the subarctic front [Roden, 1977, 1980; Lynn, 1986]. By using a large number of cross-front observations, it is possible to examine whether there are general characteristics to these temporal and spatial variations and how the frontal structure differs between the eastern and western North Pacific.

In this section, temporal and spatial variations of the strength, location, and width of the synoptic subarctic frontal zone are addressed. Mixed layer depth variations and the extent of density compensation are also investigated. Most of the data used are from discrete stations, with rather coarse resolution compared with the frontal width. Continuous underway data show how sharp an individual front can be in the frontal zone.

#### 3.1. Data

The data used in this study are CTD/STD measurements from 36 research cruises, totaling 3880 stations, in the North

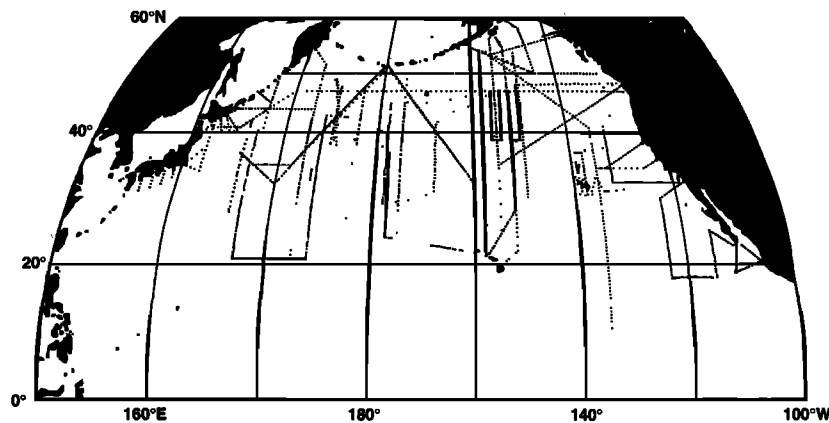


**Figure 8.** Map of conductivity-temperature-depth/salinity-temperature-depth (CTD/STD) stations used in section 3. In total, there are 3880 stations and 72 cross-front sections from 36 research cruises occupied between 1968 and 1993.

Pacific from 1968 to 1993 (Figure 8). The sources of the data are listed in Table 2. They include the surveys from the World Ocean Circulation Experiment (WOCE), International North Pacific Ocean Climate program (INPOC), Roden's [1970, 1972, 1977] frontal research, 12 years of Japanese repeated sections (JRS) [Zhang and Hanawa, 1993], the U.S. Navy's Ocean Measurement Program (OMP) [Teague, 1983], the Marathon Expedition [Martin *et al.*, 1987], hydrographic sections conducted by Woods Hole Oceanography Institute [Joyce, 1987] and NOAA Southwest Fisheries Center [Lynn, 1986], observations made from Kofu Maru, Japan (KFJAPAN), and some other individual research programs. A total of 72 cross-front sections were taken in these cruises. The data, however, are distributed unevenly in both space and time. There are more observations along 170°E, 175.5°E, and 180° than any other longitude because Japanese scientists conducted the 12 years of repeated surveys along these meridians. Relatively dense surveys are also found between 160°W and 150°W in the eastern Pacific. No observations were made in January. One section was taken each in February, March, and December. A high concentration of the data is in June and July, when the Japanese repeated surveys occur.

Most station depths are 1500 m or deeper. The vertical resolution varies from 1 to 3 m, except for the Japanese repeated sections and WOCE P13 survey (along 165°E). CTD data from JRS are stored only at standard bottle observation depths. Only bottle data from the WOCE P13 survey are available to us now. Station spacing in most surveys varies from 37 to 83 km. The spacing can be as close as 20 km or as far apart as 333 km in the subarctic frontal zone.

### 3.2. Definition of the Subarctic Front in CTD/STD Sections

In section 2.2 it was seen that the annual salinity variation at the climatological subarctic front is much smaller than the temperature variation. Therefore salinity is a relatively stable tracer to define the subarctic front. Two or three separated salinity fronts often exist in the subarctic frontal zone. The outcrop of the 33.8‰ isohaline is usually found in one of these fronts (often the southernmost one). The subarctic frontal zone retains this characteristic structure from the western North Pacific to the California Current region [Roden, 1972; Lynn, 1986]. Roden [1991] defined the subarctic frontal zone in

such a way: the outcrop of the 33.8‰ isohaline marks the southern boundary of the subarctic frontal zone. This isohaline usually forms the bottom of the permanent halocline in the subarctic gyre and outcrops in a high horizontal salinity gradient area. The outcrop of the 33.0‰ isohaline, which lies on the top of the subarctic halocline, defines the northern boundary of the frontal zone. The outcrop also occurs in a high salinity gradient area near the northern limit of the frontal zone in Roden's [1991] schematic frontal structure.

As an example, Figure 9b shows salinity structure in a meridional section along 158°W (courtesy of D. Musgrave). The 33.8‰ isohaline outcrops between station 55 and 56 (near 39.5°N), where the horizontal gradient of salinity is large. The

**Table 2.** CTD/STD Cruises Used in this Study

Program	Cruise Number	Date	Ship
WOCE	4	March 1991, June 1991, August 1992, May 1993	R/V <i>Discoverer</i> , R/V <i>Washington</i> , R/V <i>Vickers</i> , R/V <i>Thompson</i>
INPOC	6	February 1991, September 1991, October 1991, May 1992, November 1992, May 1993	R/V <i>PriLiv</i> , <i>Lavrentiev</i>
JRS	12	June–July 1978–1989	<i>Oshoro Maru</i> , <i>Hokusei Maru</i>
Roden's surveys	4	April 1968, November 1969, April 1971, September 1975	R/V <i>Thompson</i>
Marathon II	1	May 1984	R/V <i>Thompson</i>
DSJ76	1	June 1976	R/V <i>D. S. Jordan</i>
OMP	1	October 1982	USNS <i>Silas Bent</i>
WHOI	2	October 1984	R/V <i>Tompson</i>
KFJAPAN	1	May 1989	<i>Kofu Maru</i>

Many contain multiple crossings of the subarctic frontal zone, bringing the total number of crossings to 72. Abbreviations are CTD, conductivity-temperature-depth; STD, salinity-temperature-depth; WOCE, World Ocean Circulation Experiment; INPOC, International North Pacific Ocean Climate program; JRS, Japanese repeated sections; OMP, Ocean Measurement Program; WHOI, Woods Hole Oceanographic Institute; KFJAPAN, Kofu Maru, Japan.

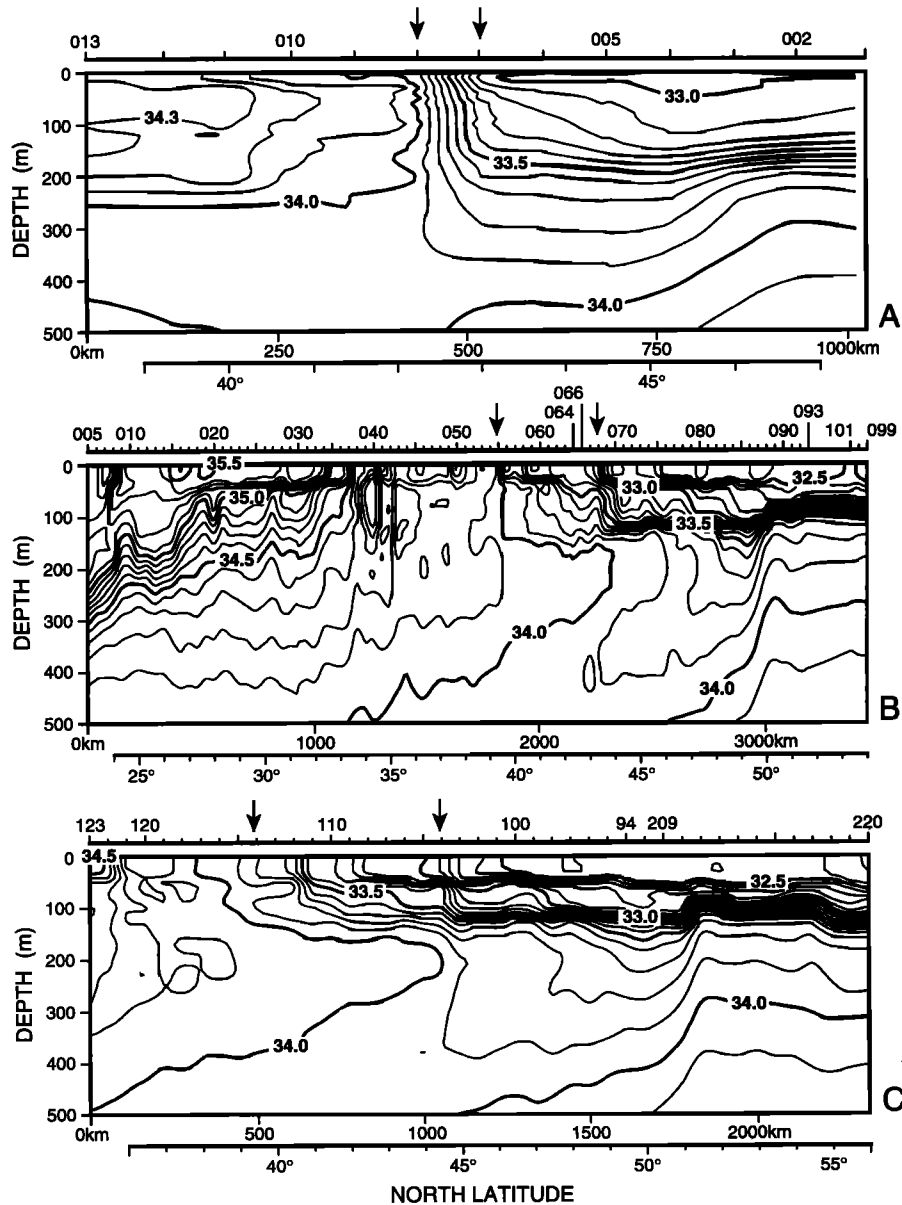


**Figure 9.** Salinity (a) along 170°E in July 1985, (b) along 158°W in September 1991, and (c) along 155°W in September 1991, as examples for the definition of the northern and southern boundaries of the subarctic frontal zone. See text for the definition. The southern and northern boundaries are indicated by arrows. The three sections show the different frontal structures.

33.0‰ isohaline outcrops between station 68 and 69 (near 43.5°N), where a relatively large horizontal gradient also exists. The southern and northern limits of the subarctic frontal zone are then clearly marked at 39.5°N and 43.5°N by Roden's definition. We use this definition to identify the southern and northern boundaries of the subarctic frontal zone in the 72 CTD/STD sections.

The salinity structure in Figure 9b is ideal for Roden's [1991] definition. However, the real ocean does not always behave as well as in Figure 9b. The outcrop of the 33.8‰ isohaline sometimes does not occur in a high horizontal gradient area. In this situation we choose the location of the highest gradient near the outcrop of the 33.8‰ instead of the outcrop itself as the southern boundary of the frontal zone, since a front is defined as an abrupt change in a tracer. The same treatment is also applied to the northern boundary when the 33.0‰ out-

crop does not occur in a high horizontal gradient area. On the other hand, the frontal zone does not always consist of two single fronts, one at each boundary. Figure 9a is an example of a single front in the frontal zone, and Figure 9c is one where the frontal zone has more than two individual fronts. We will discuss more about these frontal structures in next section.

Such defined the subarctic frontal zone is only based on salinity information and only reflects the frontal feature in the mixed layer. In the frontal zone, individual temperature fronts are not necessarily overlapping with salinity fronts. However, the mean temperature and salinity frontal zones as shown in section 2.1 and 2.2 are more or less in the same location, except in the eastern Pacific. The location and intensity of the frontal zone also can be different below the mixed layer. Readers should bear in mind the limitations of such definition in following discussion.

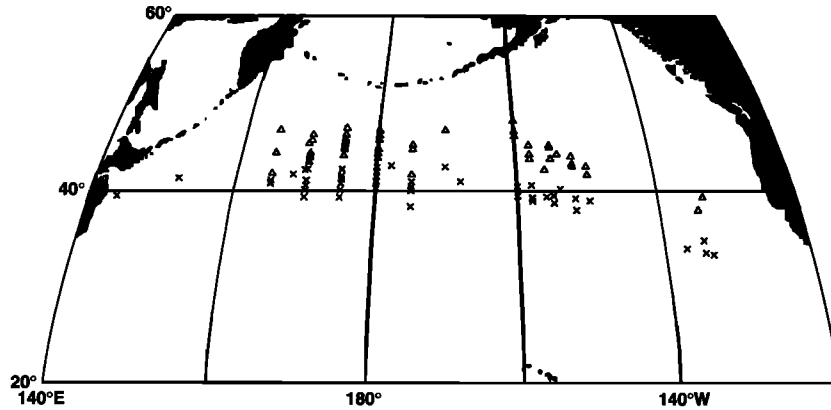


**Figure 10.** The southern (crosses) and northern (triangles) boundaries of the subarctic frontal zone defined by the outcropping of the subarctic halocline (see text) for 72 cross-front CTD/STD sections in the North Pacific.

### 3.3. The Subarctic Frontal Structure in Synoptic Surveys

The location of the subarctic frontal zone, defined as in the previous section, for each of the 72 CTD/STD sections is shown in Figure 10. In the western and central North Pacific the southern boundary of the frontal zone varies between 38°N and 44°N and the northern boundary occurs between 42°N and 47°N. The subarctic frontal zone is found between 33°N and 39°N east of 140°W. The general circulation strongly influences the location of the subarctic front. The frontal zone accompanies the North Pacific Current and the Subarctic Current across the North Pacific and then turns southward with the California Current in the eastern Pacific. The frontal location observed from the many CTD/STD sections is very close to the front in the climatological data (Figure 2b).

Temporal variation in the locations of the southern and northern boundaries is close to white noise (not shown here). The variation, as well as the annual variation of frontal position in *Levitus's* [1982] data, is relatively small compared to the width of the frontal zone. The frontal location appears to lack time dependence. This agrees with *Yoshida's* [1993] satellite observations of the temperature gradient in the western North Pacific. Because the CTD/STD data are not distributed evenly with time, seasonal variation cannot be detected. *Yoshida* [1993] reported that the position of the subarctic front does not vary seasonally in the western Pacific except in the Oyashio front region. However, *Kazmin and Rienecker* [1996] have shown that the location of the subarctic temperature front in the central North Pacific derived from satellite SST data has some seasonal variation, though the variation is much smaller than the seasonal variability of the subtropical temperature front.

Three common types of frontal structure are found in the CTD/STD data. We define a type 1 structure to be a frontal zone consisting of a single front, in other words, where the 33.0‰ to 33.8‰ isohalines all outcrop in one high surface gradient area (Figure 9a). This type of frontal structure is found on 11 sections all west of 180° in the western Pacific. Our type 2 structure consists of two individual fronts, one at each boundary of the frontal zone. Figure 9b gives an example of this type. The type 2 frontal zone is found on 28 sections without any longitudinal preference. There are more than two individual fronts in our type 3 frontal structure, two of which

usually appear at the boundaries of the frontal zone, with one or two additional fronts within the frontal zone (Figure 9c). Twenty-four sections have type 3 frontal structure. They are all east of 170°E and are frequently found in the eastern North Pacific.

The width of the subarctic frontal zone defined by salinity structure varies from 38 to 778 km (Figure 11). The variation is large. The frontal zone width is usually larger than the station spacing, so the variation of station spacing has little influence on the frontal width. The type 1 frontal structure usually has a narrower frontal zone width than the other two types of frontal structure. The mean frontal width is 400 km

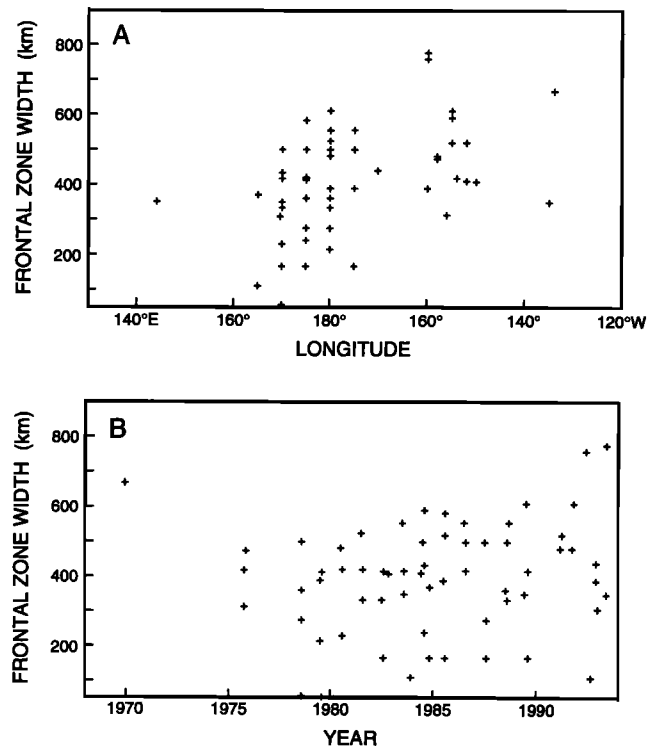


**Figure 11.** (a) Spatial and (b) temporal variations of frontal zone width in kilometers from 63 sections which completely cross the subarctic frontal zone.

with a standard deviation of 162 km. However, the frontal zone seems to be wider in the eastern Pacific than in the western Pacific. This is consistent with an origin of the subarctic front as the Oyashio front in the western North Pacific which is then advected across the Pacific; the frontal zone will be dispersed and weakened by horizontal diffusivity if local frontogenesis is not strong enough to maintain it.

Temporal variation of the frontal width has no clear pattern (Figure 11b). *Kazmin and Rienecker* [1996] showed a seasonal variation of frontal location and strength in the central North Pacific. Our data are not able to resolve the seasonal variation. Large variations of frontal width appear along Japanese repeated sections (170°E, 175°E, and 180°). Each section was usually completed in several days during June or July each year. These variations may be a interannual variation. They are also likely to reflect the results of synoptic surface forcing in the shallow mixed layer.

### 3.4. Maximum Gradients in the Frontal Zone

Temperature and salinity for the 72 CTD/STD sections were objectively mapped in the upper 1000 m and stored on a grid of 10 m in the vertical and 10 km in the horizontal. Horizontal temperature and salinity gradients in the mixed layer (at 10 m) were calculated from the gridded data. Maxima of temperature and salinity gradients within the frontal zone show the strength of individual fronts inside the frontal zone along each section. The highest value of the maxima indicates the strongest single front in each section. We use those strongest fronts in all sections to compare frontal strength across the North Pacific.

The temperature gradient of the strongest temperature front in the frontal zone from each section is plotted in Figure 12a. The mean maximum temperature gradient averaged over 72 sections is 0.44°C/10 km, which is about double *Levitus's* [1982] maximum temperature gradient shown in section 2.2. The maximum temperature gradient varies from 0.1 to 2.7°C/10 km. Most gradients are between 0.2° and 1.0°C/10 km, with an eastward decreasing trend. The warm, salty waters from the Kuroshio Current meet the cold, fresh Oyashio water in the western North Pacific. The horizontal temperature and salinity gradients are enhanced by the current system. In the eastern North Pacific the North Pacific Current splits into two branches; horizontal turbulent mixing across the front as it crosses the Pacific reduces the strength of the front.

*Roden* [1980] used satellite sea surface temperatures (SST) obtained from Gosstcomp to calculate the intensity of the subarctic front in the western North Pacific. The satellite data were averaged spatially over 100 km by 100 km squares and temporally over a week. His maximum meridional temperature gradient from March 1977 to March 1978 was 0.5°C/10 km in March 1977. His maximum temperature gradient is about the same magnitude as the mean maximum gradient in our data but is much smaller than the strongest temperature front in the CTD/STD data due to the spatial sampling. Another independent measurement of the subarctic frontal strength is by *Kazmin and Rienecker* [1996] for the central North Pacific. He used weekly composite SST at 18-km resolution from 1982 to 1992 produced by the University of Miami/Rosenstiel School of Marine and Atmospheric Sciences (RSMAS) from satellite multichannel advanced very high resolution radiometer (AVHRR) measurements. His temperature gradient is calculated from zonally averaged SST and then smoothed with a 4-week running average. The resulting maximum temperature gradient varies between 0.08° and 0.18°C/10 km, which is even

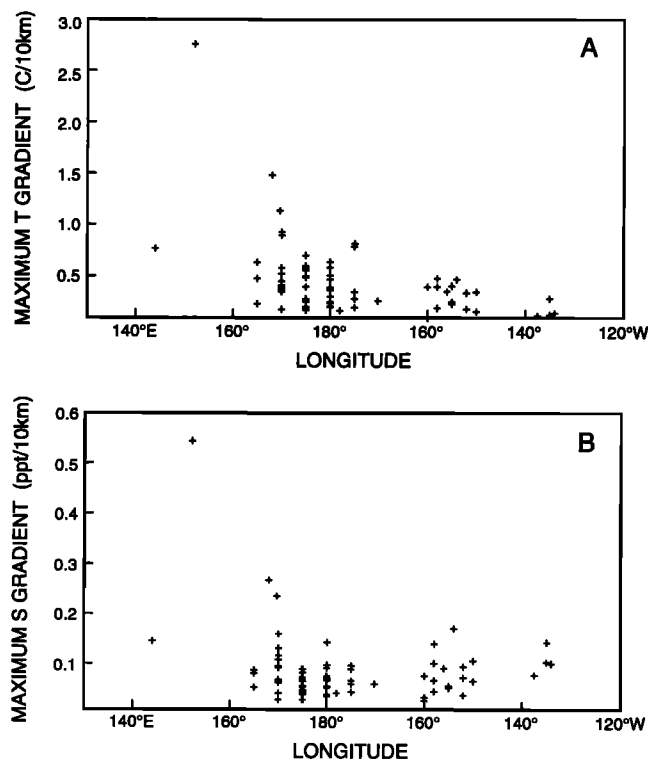


**Figure 12.** (a) Maximum temperature and (b) maximum salinity gradients at 10-m depth in the subarctic frontal zone as functions of longitude. Units are degrees Celsius per 10 km and parts per thousand per 10 km for temperature and salinity, respectively.

smaller than *Roden's* observation. The magnitude of the maximum gradient of those individual fronts in our data set is relatively higher than the above two satellite observations. The main reason for this difference in magnitude is that our CTD/STD sections are synoptic and are not averaged spatially or temporally.

Temporal variation of the maximum temperature gradient based on CTD/STD sections is also close to white noise. Uneven sampling of the data in time might cause this. However, *Kazmin and Rienecker* [1996] found a clear seasonal signal with maximum in summer in the strength of the subarctic front in the central North Pacific.

The maximum salinity gradient in the frontal zone is shown in Figure 12b. The maximum gradient varies from 0.03 to 0.3‰/10 km, except in one observation along 152°E where it reaches 0.55‰/10 km. The highest temperature gradient also occurred on the same section which was made in May 1982. The mean maximum salinity gradient over 72 sections is 0.087‰/10 km, which is 4 times *Levitus's* maximum salinity gradient in the subarctic front. Again, no seasonal or interannual variation is observed in the maximum salinity gradient. We do not know any other independent data to compare with our CTD/STD data on the strength of the salinity front in the subarctic frontal zone.

Although the maxima of the temperature and salinity gradients in our CTD/STD data are higher than the satellite observations mentioned above, they are still derived from the sections whose mean station spacing is 66 km. An individual oceanic front is expected to have a length scale much smaller than this station spacing. We also should bear in mind that

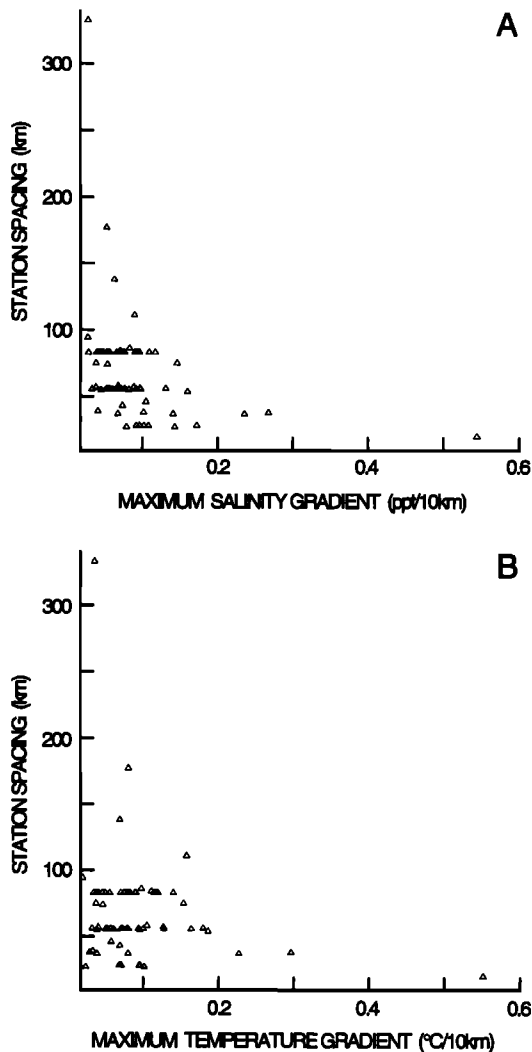


**Figure 13.** (a) Maximum salinity and (b) maximum temperature gradients in the subarctic frontal zone as functions of the station spacing near the frontal zone for each of the CTD/STD surveys. The mean station spacing over the 72 sections is 66 km.

station spacing strongly influences the horizontal maximum gradients of tracers. Figure 13 shows the relationship between the maximum temperature/salinity gradient and the station spacing. The station spacing varies from 20 to 333 km in the 72 sections. Most surveys have station spacings of 83, 55, or around 30 km. Larger temperature and salinity gradients tend to occur when the station spacing is small. The strength of the individual fronts also varies with time and location. It is not expected to be a linear function of the station spacing. Nevertheless, inadequate sampling in space will not give accurate frontal strengths. Fortunately, the station spacings do not have an eastward increasing trend. Therefore the eastward decreasing trend in the maximum temperature gradient is probably accurate.

Surface temperatures were collected continuously along the WOCE P17 section, which is one of our 36 CTD/STD cruises. The cruise occupied the southern part of the subarctic frontal zone along 135°W. The southern boundary of the frontal zone is located at 33.57°N from the CTD section. A temperature probe was mounted on the ship at an inlet about 2–3 m below the sea surface. Temperature was continuously recorded and

averaged every minute. Raw underway temperature data from 34.6°N to 30.0°N are shown in Figure 14. Three individual fronts occur near 180, 300, and 550 km along the section. The front near 180 km is within the subarctic frontal zone derived from the CTD station data. The true front as seen in the underway data has a temperature contrast of 0.94°C and a width of 8 km. This frontal strength is equivalent to a horizontal temperature gradient of 0.11°C/km, which is roughly 10 times the gradient of the same front observed from the discrete CTD station data spacing at 55 km. *Samelson and Paulson* [1988] observed the same phenomenon in the subtropical front. The subtropical front near 30.5°N (distance 550 km) is the strongest of the three. This front has a strength of 0.20°C/km. The spikes in the underway temperature mark the locations of CTD stations. (When a ship stopped at a station, the surface temperature near the inlet may be warmed up by the ship.) The temperature measured at the CTD stations is much smoother than the underway temperature, due to the coarse sampling density.

### 3.5. Stability Gap in Synoptic Surveys

A stability gap has been found in CTD/STD sections [*Roden*, 1970, 1972] and in *Levitus's* [1982] winter data (see section 2.3). As mentioned in section 2.3 this lateral minimum in the vertical stability maximum at the mixed layer base is due to the locally weak permanent thermocline and the outcropping of

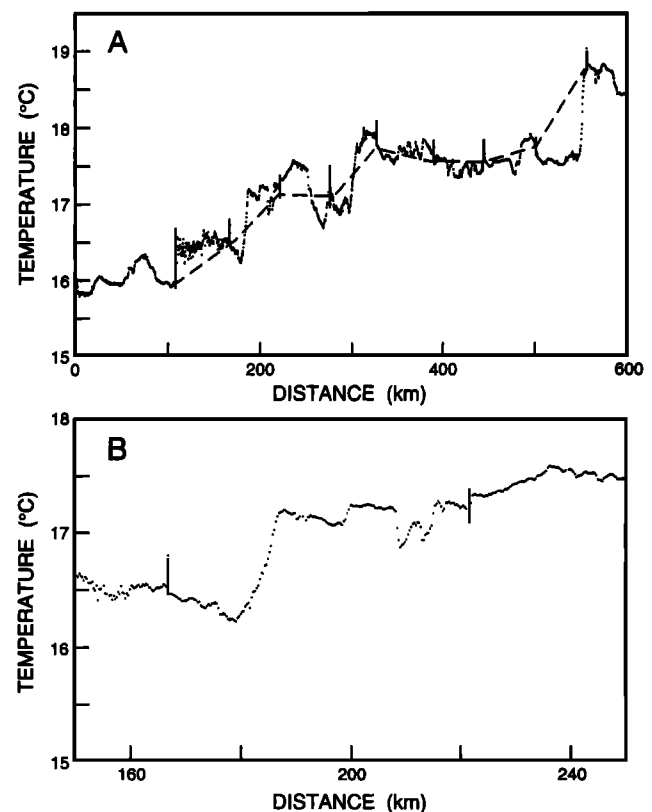


**Figure 14.** (a) Underway temperature from 34.6°N to 30.0°N along 135°W in June 1991. Heavy dashed line is a contour of the sea surface temperature from the temperature at CTD stations. (b) A single front at 33.75°N (near distance 180 km) within the subarctic frontal zone defined by salinity structure from CTD station data.

the subarctic permanent halocline. In this section we examine the stability gap from our collected CTD/STD sections.

The stability gap is found south of the subarctic front in the six CTD/STD sections which were taken between February and April. The sections were along 152°W, 158°W, 160°W, 168°W, 178°W, and 168°E. In these winter months when the seasonal thermocline is also absent, vertical mixing can penetrate deeper in the stability gap than in the subarctic gyre to the north and in the subtropical gyre to the south.

A shallow thermocline starts to build up from south to north during May. Six sections were taken in May. Three of them, which were along 152°W and 160°W, extended to both the subarctic and subtropical gyres. A shallow stable layer at the surface appears south of the stability gap or south of the subarctic front, but not north of the front, along these three sections. The other two May sections were taken along 152°E and 144°E in the western Pacific. Neither extended to the subarctic gyre. Maximum stability occurs at the surface along these two western sections. The last section taken in May (WOCE P17N, along 135°W, courtesy of D. Musgrave) did not extend south of the subarctic frontal zone. No shallow or surface stable layer exists north of the subarctic front. In general, we start to see the surface or shallow stable layer in May south of the subarctic front. The seasonal thermocline is established in both the subtropical and subarctic gyres from June to December basinwide. The shallow stable layer caused by the thermocline then caps the winter stability gap. However, the horizontal minimum of the vertical stability near 200 m south of the subarctic frontal zone remains in all seasons.

### 3.6. The Mixed Layer Depth Across the Frontal Zone

The existence of the stability gap south of the subarctic frontal zone may affect the mixed layer depth across the frontal zone. We define the depth of the vertical maximum of Väisälä frequency as the mixed layer depth. Ten out of 12 sections taken between February and May extend at least across the southern boundary of the subarctic frontal zone and are used to examine the mixed layer depth across the front. Eight of them have southward mixed layer deepening over a couple degrees of latitude either south of the frontal zone or starting within the frontal zone. The eight sections were all taken east of 168°E. The deepening of the mixed layer depth varies from 30 to 260 m. The other two sections were occupied along 144°E and 152°E in the western boundary current region. The most stable layer is found at the surface in both sections. No well-defined mixed layer exists along these sections.

Figure 15 shows the mixed layer depth on a salinity section along 152°W in May 1984. The mixed layer depth coincides with the top of the permanent halocline north of the southern boundary of the subarctic frontal zone. The depth is about 100 m within the frontal zone. The mixed layer deepens southward immediately south of the southern boundary of the frontal zone. The 40-m deepening occurs in less than a degree of latitude in the stability gap. The mixed layer depth suddenly decreases to the south at 38.5°N due to a seasonal thermocline in the subtropical gyre.

To examine the effect of wind stress curl on the mixed layer deepening within and south of the subarctic front, Ekman pumping is calculated for May 1984 using monthly mean Fleet Numerical Oceanography Center (FNOC) wind stress. Zero Ekman pumping occurs near the northern boundary of the frontal zone, which is about 400 km north of the onset of mixed layer deepening. So the Ekman pumping is probably not di-

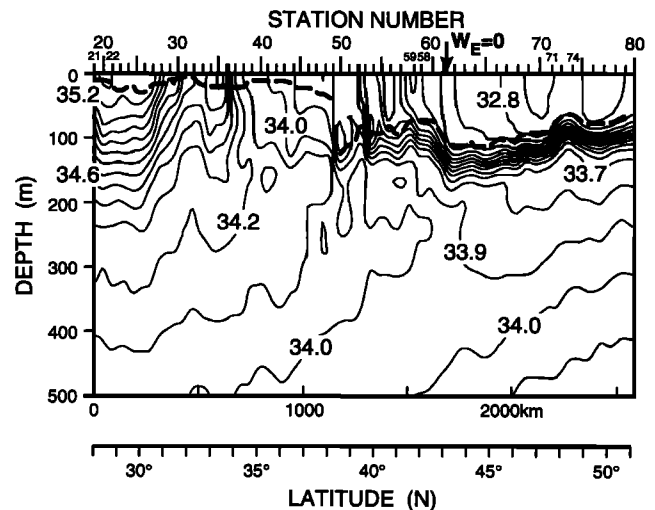


**Figure 15.** Salinity along 152°W in May 1984. The heavy dashed line shows the mixed layer depth defined by the maximum Väisälä frequency in vertical. The arrow shows where the monthly mean vertical Ekman velocity equals zero in May 1984. The southern boundary of the subarctic frontal zone occurs near station 52.

rectly related to the mixed layer deepening south of the subarctic frontal zone. The mixed layer deepening is related to the outcrop of the subarctic halocline.

The mixed layer along 152°W (Figure 15) has a similar amount of deepening near the northern boundary of the frontal zone. The northern deepening occurs near the zero Ekman pumping. However, Ekman suction to the north and Ekman pumping to the south tend to tilt the mixed layer base in the opposite direction. Thus Ekman pumping cannot generate this northward deepening either.

What causes the outcrop of the subarctic halocline is not fully understood yet. *Yuan and Talley* [1992] showed that long-term mean zero Ekman pumping crosses the subarctic front in the central North Pacific. The outcrop of the subarctic halocline is in a mean Ekman divergent area in the western Pacific and in a mean Ekman convergent area in the eastern Pacific. So the long-term mean Ekman pumping is not the mechanism that makes the subarctic halocline outcrop. Excessive evaporation over precipitation in the subtropical gyre can make the surface salinity as high as the salinity at the subarctic halocline and help to bring the subarctic halocline up to the surface. The outcrop of the subarctic halocline is possibly determined by the water mass distribution and the general circulation in the North Pacific.

We do not have enough winter CTD/STD sections to create a geographic distribution of mixed layer depth. As shown in section 2.3 the mixed layer depth can reach to more than 200 m in the stability gap. The deepening is especially fast at the boundary of the gap. In recent studies, Nakamura (submitted manuscript, 1996) and Suga et al. (submitted manuscript, 1996) suggested that the North Pacific Central Mode Water is formed in this stability gap due to deeper winter convection and advected away from its formation area by general circulation. Our data suggest that the subarctic frontal zone can serve as the northern limit of the formation area of this Central Mode Water.

Bear in mind, this mixed layer deepening can cause a con-

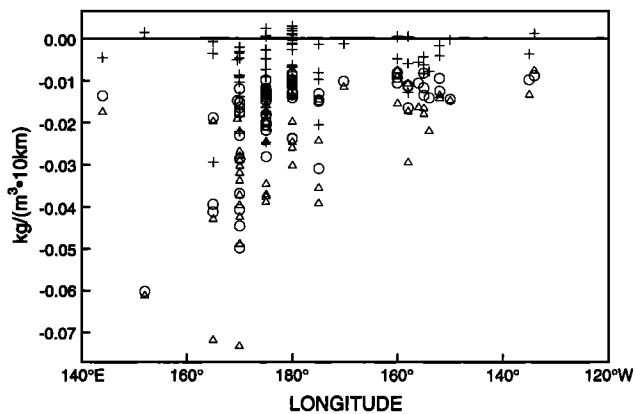


**Figure 16.** Mean  $\alpha\partial_y T$  (triangles),  $\beta\partial_y S$  (circles), and  $\partial_y \sigma_\theta$  (crosses) at 10-m depth in the subarctic frontal zone from 63 complete cross-front CTD/STD sections. Units are kilograms per cubic meter per 10 km.

vergence of the Ekman velocity regardless of whether it occurs in an Ekman transport convergent area or in a divergent area, since the westerlies always generate southward Ekman transport in this region. The convergence of the Ekman velocity is one frontogenetic mechanism. A detailed analysis about the effect of wind stress on the subarctic front will be presented in a following paper.

### 3.7. Density Compensation in the Frontal Zone

Weak density gradients and strong, compensated temperature and salinity gradients have been observed in the subarctic front [Roden, 1972, 1975, 1977]. We use the same method which was applied to the *Levitus* [1982] data in section 2.4 to examine and quantify the density compensating nature of the subarctic front using synoptic data. Horizontal temperature and salinity changes over 10 km ( $\alpha\partial_y T$  and  $\beta\partial_y S$ ) were calculated in density units along 63 complete cross-front sections and then smoothed by a Gaussian filter of 2° latitude width. Again, longitudinal gradients are neglected because of their smallness. Mean  $\alpha\partial_y T$  and  $\beta\partial_y S$  in the frontal zone were obtained by averaging between the southern and northern boundaries. Density ratio ( $R_\rho = \alpha\Delta T/\beta\Delta S$ ) and Turner angle (see section 2.4 for definition) are also calculated, smoothed horizontally, and averaged within the subarctic frontal zone.

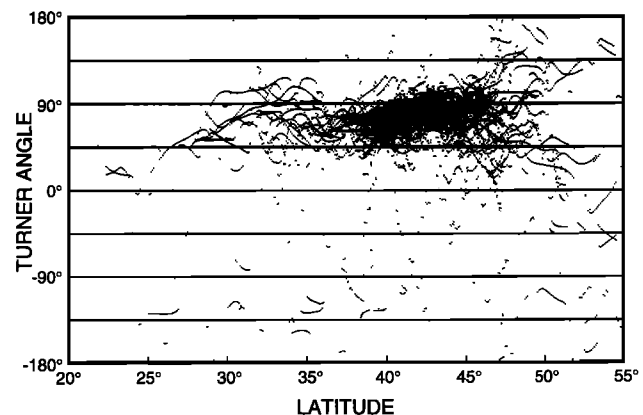
The mean  $\alpha\partial_y T$  and mean  $\beta\partial_y S$  are compared with mean density change in the frontal zone (Figure 16). In most sections, weak density gradients exist, although they are usually smaller than either temperature or salinity gradients. The temperature gradients are often the largest. Occasionally, the temperature and salinity gradients completely compensate each other, with the resulting density gradient equal to zero. Large temporal variations exist along 170°E, 175°E, 180°, and 175°W because repeated surveys were done along these longitudes. The largest density gradient is found along 165°E, which was taken in August 1992. The two other surveys along the same longitude were taken in November 1983 and October 1984 and show relatively small density gradients. The synoptic observations along 165°E are consistent with *Levitus's* [1982] data in the aspect of less density compensation during summer months (Figure 7B).

Mean Turner angle in the frontal zone averaged over 63 sections is 78.3°, with a standard deviation of 11.1°. The mean

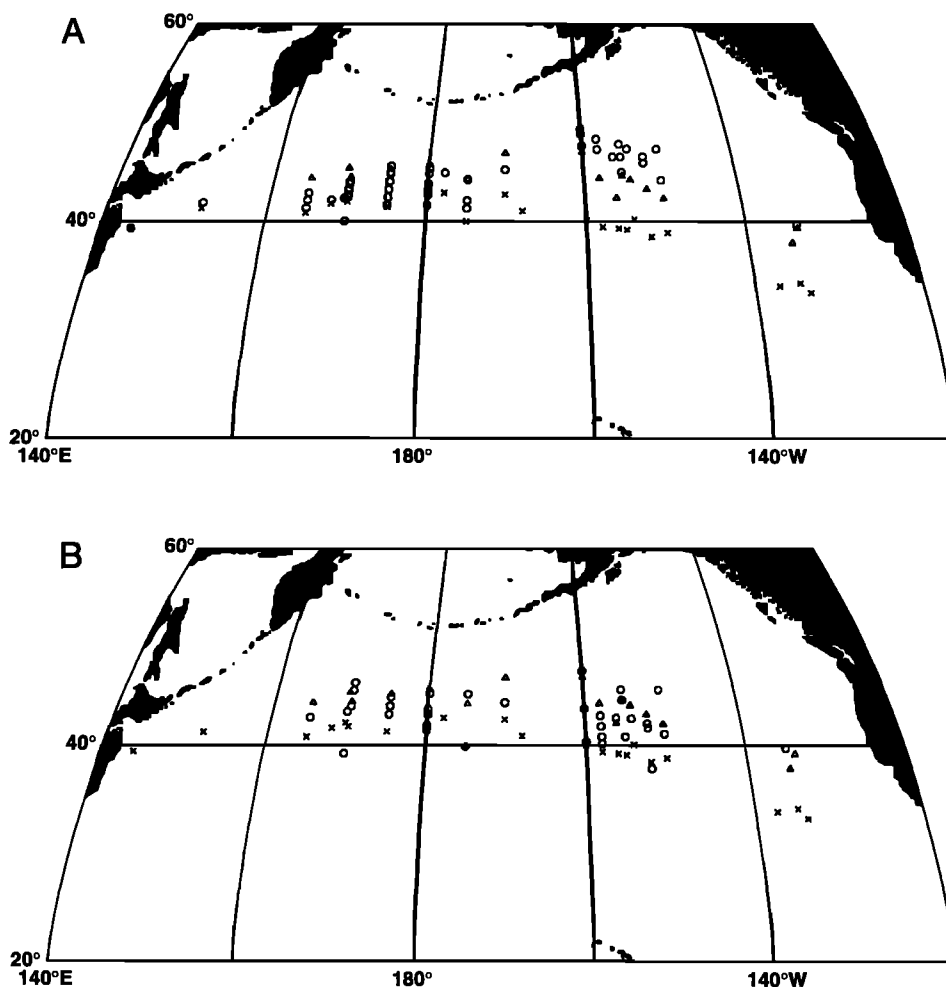
Turner angle falls in temperature-dominated regime (see Figure 6). This mean Turner angle is equivalent to a density ratio of 2.08 which is about the mean density ratio in the midlatitude North Pacific (about 30 to 50°N) [Stommel, 1993; Chen, 1995]. In general, the subarctic frontal zone is partially density compensated.

Figure 17 shows Turner angles along 72 sections. Even though the CTD/STD temperature and salinity are smoothed with a Gaussian filter of 2° latitude width, the Turner angles are still much noisier than the those calculated from *Levitus's* [1982] data (Figure 7). The Turner angles cluster between 70° and 90° from 39° to 47°N, where the subarctic frontal zone occurs. Between 27° and 38°N the Turner angles are more evenly distributed between 45° and 120°. However, the Turner angles in the climatological data are all smaller than 90° in this area. North of 47°N, the Turner angles start to become larger than 90° and smaller than 45°, showing salt dominance. The pattern is similar to the climatological data in the subarctic ocean.

The subarctic frontal zone consists of one to several temperature and salinity fronts. The horizontal temperature and salinity gradients between the fronts are much weaker than at the fronts. The weak salinity gradients can generate very large density ratios. These weak gradients bring the cross-frontal-zone averaged density ratio to the background level. They also cause the noisy Turner angles within the frontal zone (Figure 17). To investigate how much the density gradient is compensated at the individual fronts, we choose the strongest available temperature and salinity fronts within the subarctic frontal zone from each section. The strongest salinity front may not occur at the same place of the strongest temperature front in the same section. Density ratio is calculated at these fronts without horizontal smoothing and then averaged over 72 sections. The mean density ratio at the strongest temperature fronts is 2.10, which is very close to the cross-frontal-zone average. The standard deviation of this mean is 3.69, implying very large variations between the sections. The mean density ratio at the strongest salinity fronts is 0.96 with a relatively smaller standard deviation of 0.51. The density gradient tends to be more compensated at the strongest salinity fronts than at the strongest temperature fronts.



**Figure 17.** Turner angles along 72 CTD/STD sections. Temperature and salinity are horizontally smoothed with a Gaussian filter of 2° latitude width before calculating the Turner angles. Most of the angles are between 45° and 90° in the latitude range of 25° to 45°N, which agrees with *Levitus's* [1982] data in section 2.4, although the synoptic data are much noisier.



**Figure 18.** (a) The northern boundary of the North Pacific Intermediate Water (circles) relative to the northern (triangles) and southern (crosses) boundaries of the subarctic frontal zone. (b) The northern onset of the shallow salinity minimum (circles) relative to the southern (crosses) and northern (triangles) boundaries of the subarctic frontal zone.

### 3.8. The Subarctic Front Relative to the NPIW and SSM

The North Pacific Intermediate Water (NPIW), indicated by a well-defined, thick, and smooth salinity minimum, occurs in the density range of 26.7 to 26.9  $\sigma_\theta$  throughout the subtropics [Reid, 1965; Talley, 1993]. The NPIW centers around a depth from 500 to 700 m in the subtropical gyre. The presence of the NPIW characterizes the subtropical water. On the other hand, the subarctic frontal zone is usually regarded as a boundary between the subarctic and subtropical gyres in the upper ocean. The northern boundary of the NPIW relative to the subarctic frontal zone is shown in Figure 18a. The NPIW appears north of the northern boundary of the frontal zone in the eastern North Pacific. However, it merges with the frontal zone west of 170°W. The sloping of the northern boundary of the NPIW relative to the northern boundary of the subarctic frontal zone suggests that the subarctic water extends southward in the uppermost layer and lies above the subtropical water in the eastern North Pacific. In other words, the gyres “water mass boundary” is shifted northward with depth in the eastern North Pacific. This is likely due to southward Ekman transport of the surface layer relative to the eastward general circulation so that subpolar surface waters are advected south-

ward over the subtropical waters in the eastern Pacific. Such vertical tilting of the gyre boundary does not occur in the central and western North Pacific.

The shallow salinity minimum (SSM) is observed at 25.1 <  $\sigma_\theta$  < 26.2 and above the NPIW in the eastern North Pacific south of 50°N [Reid, 1973; Tsuchiya, 1982; Yuan and Talley, 1992]. The potential role of the frontal zone in creation of the SSM was mentioned but not demonstrated by Talley *et al.* [1991] and Yuan and Talley [1992]. Using the CTD/STD data set, we are able to compare the location of the onset of the SSM with the subarctic frontal zone (Figure 18b). The SSM starts within the subarctic frontal zone. The SSM occasionally starts north of the northern boundary but usually does not start south of the southern boundary. This implies that the subarctic front is important in the formation of the SSM. At the least the front limits the source water area of the SSM.

### 3.9. Differences Between the Western and Eastern North Pacific

Differences exist in the subarctic front between the western and eastern North Pacific in both climatological data and the synoptic surveys. The climatological temperature frontal zone and individual temperature fronts in the frontal zone are stron-

ger in the western Pacific than in the eastern Pacific. The width of the frontal zone is narrower in the west than in the east. Our type 1 frontal structure, in which the northern and southern boundaries of the frontal zone merge together to form a single front, is often found in the western Pacific but never in the eastern Pacific. Our type 3 frontal structure which includes more than two individual fronts is more frequently found in the eastern North Pacific.

Another characteristic of the subarctic front is its depth which varies significantly across the North Pacific. West of 165°E (including 165°E), the salinity front can penetrate down from 350 to more than 800 m. However, the depth varies from 180 to only 400 m east of 165°E. The longitudinal variation of the temperature front depths is less than the salinity fronts. Density fronts usually exist in the subarctic frontal zone below the mixed layer across the North Pacific, even though they are quite weak in the mixed layer. The density fronts, as well as associated baroclinic currents, are much stronger in the western boundary current region than in the rest of the North Pacific.

#### 4. Discussion

We hypothesize that the subarctic front is initiated at the Oyashio front in the western North Pacific and advected across the North Pacific by the North Pacific Current and the Subarctic Current. In the eastern boundary current region the subarctic temperature and salinity fronts turn southward with the California Current. The southward turning fronts are observed in both *Levitus's* [1982] data and synoptic surveys [Lynn, 1986]. *Levitus's* [1982] temperature data also show a northward turning branch in the eastern North Pacific. However, there are insufficient synoptic observations to confirm the northward turning temperature front. Horizontal turbulent mixing should tend to disperse and weaken the front on its approximately 6000 km journey across the ocean. Our data show that the frontal zone is narrower and individual fronts are relatively stronger in the west than in the east, which are supportive of this hypothesis. Nevertheless, sufficient local frontogenesis along its path is needed to maintain the sharpness of individual fronts.

*Roden* [1977] suggested that the following four processes cause frontogenesis in the open ocean: (1) convergence of horizontal advection upon non-uniformly distributed temperature and salinity, (2) horizontal variation of vertical advection, (3) horizontal variations of nonturbulent heat and salt fluxes at the surface, and (4) horizontal variation of turbulent fluxes. His results showed that Ekman convergence and horizontal variation of the Ekman pumping are the main sources of subarctic frontogenesis during fall in the eastern North Pacific. The surface nonturbulent and turbulent fluxes are not important in fall.

*Kazmin and Rienecker* [1996] also showed the importance of the first three frontogenesis mechanisms in the central North Pacific. They showed that the sum of Ekman convergence and meridional derivative of surface heat flux has a significant seasonal variability. Its maximum occurs near the subarctic front during summer and moves to south of 30°N in winter. Frontogenesis due to the meridional variability of Ekman pumping (from wind stress and *Levitus's* data) also has a maximum near 42°N only in summer.

The strong seasonal signal in the above frontogenetic terms does not match the relatively stable frontal location. The three processes that *Kazmin and Rienecker* [1996] showed may be the major frontogenesis mechanisms during summer. Different

processes have to be considered for other seasons. Unevenly distributed turbulent flux is another frontogenetic mechanism. In a following paper a wind stress analysis will show that the energy at synoptic timescales has a high meridional gradient across the subarctic front especially in the western North Pacific. *Roden* [1977] parameterized convective turbulent fluxes and showed that they cause frontolysis in the subarctic frontal area. However, other forms of turbulent mixing, such as wind stirring in the mixed layer and entrainment at the base of the mixed layer, can be frontogenetic. These two forms of turbulent mixing are directly related to the wind stress at the synoptic timescale.

The most important factor in forming the subarctic front is the outcrop of the subarctic permanent halocline. This outcrop is so prominent that we use the outcrops to define the frontal zone. In the western North Pacific the salty water from the Kuroshio meets the fresh Oyashio water in the mixed water region, creating a high surface salinity gradient. A strong temperature contrast is also created by the northward moving warm water and the southward moving cold water in the western boundary current region. When the Oyashio separates from the western boundary, the accompanying high surface temperature and salinity gradients are advected eastward. If there is enough frontogenesis to maintain the high temperature and salinity contrasts, they will be advected across the North Pacific as a major frontal zone.

Unlike the mean temperature front in the *Levitus's* data the mean salinity front is not weakened eastward. In the synoptic sections the strongest individual salinity fronts weaken less toward the east than the strongest temperature fronts. This implies that salinity frontogenesis is relatively stronger than temperature frontogenesis in the eastern North Pacific. As we know the lowest surface salinity is found in the eastern subpolar gyre due to excess runoff and precipitation there. This may cause the meridional salinity gradient across the gyre boundary to be stronger in the eastern Pacific than in the western Pacific. In the eastern Pacific, both the Ekman advection and geostrophic flow contribute to transport the surface subarctic water into the subtropical gyre, where it meets the high-salinity subtropical surface water. This enhances the subarctic salinity front. On the other hand, the meridional temperature gradient across the gyre boundary is weaker in the eastern Pacific than in the western Pacific. The same amount of subarctic surface water flushed into the subtropical gyre will create less temperature gradient than salinity gradient. So local frontogenetic processes should be more favorable to the salinity front in the eastern Pacific. As shown in section 2.4 the subarctic front occurs in the transition area between temperature-dominated regime and salinity-dominated regime in the western and central Pacific. It, however, appears south of the transition area in the eastern Pacific (Figure 7). The stronger salinity front generates a small density gradient in the frontal zone even though the frontal zone occurs in the temperature-dominated regime (Figure 7). That explains why the subarctic front is in the temperature-dominated regime yet is still density compensating in the eastern Pacific.

#### 5. Summary

The analysis in this study provides a climatological background for the subarctic frontal zone and detailed structure of the frontal zone based on the synoptic surveys. The position and shape of the climatological frontal zone may not agree

with synoptic observations due to the heavy smoothing in *Levitus's* [1982] data and time dependence. Major characteristics of the mean frontal zone in *Levitus's* [1982] data are summarized as following.

The subarctic frontal zone is a well-defined temperature and salinity front across the North Pacific in the heavily smoothed *Levitus* [1982] data. It is located between 40°N and 44°N in the western and central Pacific. The subarctic temperature front splits into two branches in the eastern Pacific. One branch turns northward and the other turns southward. The subarctic salinity front turns southward and combines with the subtropical front in the eastern Pacific due to the smoothing applied to the data.

The strength of the subarctic temperature front is strongest in the western Pacific and decreases eastward. The annual variation of the strength of the front is also stronger in the western and central Pacific than in the eastern Pacific. The front moves only a few degrees of latitude annually. This annual variation of the frontal location is comparable to the width of the frontal zone.

The subarctic salinity front has relatively smaller variation in strength across the Pacific. It also moves a few degrees of latitude annually. The smallest annual variation in both strength and position can be found in the central Pacific.

Temperature at the subarctic temperature front can vary up to 10.44°C annually, which is much larger than the temperature change across the front. Salinity at the salinity front has an annual variation of 0.23‰, which is comparable to the salinity change across the front.

A hydrostatic stability gap at the base of the mixed layer exists south of the subarctic front in winter because of the absence of a permanent halocline and seasonal thermocline. It is bounded by the permanent thermocline in the subtropical gyre to the south. The stability gap can be found basinwide.

The subarctic frontal zone in the western and central Pacific occurs in a transition area, where horizontal temperature and salinity gradients contribute roughly equally to the horizontal density gradient. Temperature gradients dominate to the south in the subtropical ocean, while salinity gradients dominate to the north in the subarctic ocean. This climatological background of temperature and salinity structure offers a favorable condition for formation of density compensating fronts in the subarctic frontal zone. In the eastern Pacific the frontal zone occurs in the temperature-dominated regime. The density gradient is also weak in the frontal zone due to the existence of the strong salinity front. The low-salinity subarctic water is flushed into the subtropical gyre in the upper ocean and meets the high-salinity subtropical surface water in the eastern Pacific, which enhances the salinity front in the temperature-dominated regime.

The subarctic frontal zone in the synoptic surveys shows a variety of detailed structures even as it retains many the characteristics from the climatological data. Although those detailed frontal structures may be strongly influenced by local synoptic weather systems, they do have some common characteristics across the Pacific. The main characteristics from synoptic observations are summarized as follows.

The subarctic frontal zone in CTD/STD sections is well defined by its salinity structure, the outcropping of the subarctic halocline. Three types of frontal structure are found: a single front, one individual front at each of two boundaries, and more than two fronts in the frontal zone. The first is found in the western North Pacific, while the last often appears in the

eastern North Pacific. The double frontal structure does not have longitudinal preference.

The width of the subarctic frontal zone increases eastward with much scatter. The mean frontal width averaged over 63 sections which completely crossed the frontal zone is about 400 km. In general, the frontal width is equivalent to or larger than the annual migration of the frontal location shown in the *Levitus's* [1982] data. Temporal variations exist in frontal location, frontal width, and maximum gradients within the frontal zone from CTD/STD sections. The temporal variations have no clear pattern and include all synoptic, seasonal and interannual variations which cannot be distinguished based upon our CTD/STD data set.

Random local atmospheric forcing strongly influences the strength of individual fronts, so that the temporal variations of maximum temperature and salinity gradients within the frontal zone are large and random. However, the strength of individual fronts does have a spatial pattern. The maximum temperature gradient is larger in the western Pacific than in the eastern Pacific. The eastward decrease in the strength of the salinity fronts is less significant than for the temperature fronts.

Averaged maximum temperature and salinity gradients in the subarctic frontal zone from the CTD/STD sections are 2–4 times the maximum gradients from *Levitus's* [1982] averaged data. However, the strength of an actual single temperature front measured from continuous data can be about 10 times the strength of the same front measured using discrete stations at standard spacing for large-scale circulation studies. Although those discrete station measurements are not adequate to resolve individual fronts, they do show the vertical structure of the frontal zone.

Similar to the climatological frontal zone, the frontal zone in synoptic data largely occurs at the transition area between gyres. Temperature gradients dominate to the south in the subtropical gyre, while salinity gradients dominate to the north in the subpolar gyre. Density gradients tend to be more completely compensated at the strongest individual salinity fronts than at the strongest temperature fronts in the subarctic frontal zone. The mean density ratio at the strongest salinity fronts is 0.96, and the mean density ratio at the strongest temperature fronts (2.10) is very close to the background density ratio in the midlatitudes (30° to 50°N).

The mixed layer deepens southward south of or within the frontal zone in winter and spring. The deepening occurs just south of the outcrop of the subarctic permanent halocline in the subarctic frontal zone.

The subarctic frontal zone limits the source water area of the shallow salinity minima to the north of the front in the eastern Pacific. It also limits the formation area of the North Pacific Central Mode Water to the south of the front. The frontal zone is found south of the northern boundary of the North Pacific Intermediate Water in the eastern Pacific, which indicates the subarctic water lies above the subtropical water in that area.

The frontal structure and the relatively narrower frontal width and stronger frontal strength in the western Pacific than in the eastern Pacific suggest an hypothesis: The subarctic frontal zone originates from the Oyashio front in the western Pacific and is advected across the North Pacific by the general circulation. Horizontal mixing and diffusivity tend to disperse and weaken the frontal zone on its way across the ocean. On the other hand, local frontogenetic processes, such as Ekman

convergence, can generate sharp individual fronts inside the frontal zone and help to maintain the frontal zone.

**Acknowledgments.** The authors thank G. Roden, R. Lynn, D. Musgrave, T. Joyce, P. Niiler, and S. Ignell for providing CTD/STD data. This work was supported by the National Science Foundation Ocean Sciences Division under grants OCE-8658120 and OCE92-03880.

## References

- Camerlengo, A., Large-scale response of the Pacific Ocean subarctic front to momentum transfer: A numerical study, *J. Phys. Oceanogr.*, **12**, 1106–1121, 1982.
- Chen, L. G., Mixed layer density ratio from the Levitus data, *J. Phys. Oceanogr.*, **25**, 691–701, 1995.
- Dodimead, A. J., F. Favorite, and T. Hirano, Review of oceanography of the subarctic Pacific region, *Bull. Int. N. Pac. Comm.*, **13**, 195 pp., 1963.
- Joyce, T. W., Hydrographic sections across the Kuroshio extension at 165°E and 175°W, *Deep Sea Res., Part A*, **34**, 1331–1352, 1987.
- Kazmin, A. S., and M. M. Rienecker, Variability and frontogenesis in the large-scale oceanic frontal zones, *J. Geophys. Res.*, **101**, 907–921, 1996.
- Levitus, S., *Climatological atlas of the world ocean*, NOAA Prof. Pap., **13**, 149 pp., 1982.
- Lynn, R. J., The subarctic and northern subtropical fronts in the eastern North Pacific ocean in spring, *J. Phys. Oceanogr.*, **16**, 209–222, 1986.
- Martin, M., L. D. Talley, and R. A. de Szoeko, Physical, chemical and CTD data from the Marathon Expedition, R/V Thomas Washington 261, *Oreg. State Univ. Ref.*, **87-15**, 213 pp., 1987.
- Mizuno, K., and W. B. White, Annual and interannual variability in the Kuroshio current system, *J. Phys. Oceanogr.*, **13**, 1847–1867, 1983.
- Reid, J. L., *Intermediate waters of the Pacific Ocean*, Johns Hopkins Oceanogr. Stud., **2**, 85 pp., 1965.
- Reid, J. L., The shallow salinity minima of the Pacific ocean, *Deep Sea Res.*, **20**, 51–68, 1973.
- Reid, J. L., On the use of dissolved oxygen concentration as an indicator of winter convection, *Nav. Res. Rev.*, **34**, 28–39, 1982.
- Roden, G. I., Shallow temperature inversions in the Pacific Ocean, *J. Geophys. Res.*, **69**, 2899–2914, 1964.
- Roden, G. I., Aspects of the mid-Pacific transition zone, *J. Geophys. Res.*, **75**, 1097–1109, 1970.
- Roden, G. I., Temperature and salinity fronts at the boundaries of the subarctic-subtropical transition zone in the western Pacific, *J. Geophys. Res.*, **77**, 7175–7187, 1972.
- Roden, G. I., Thermohaline structure, fronts, and sea-air energy exchange of the trade wind region east of Hawaii, *J. Phys. Oceanogr.*, **4**, 168–182, 1974.
- Roden, G. I., On the North Pacific temperature, salinity, sound velocity and density fronts and their relation to the wind and energy flux fields, *J. Phys. Oceanogr.*, **5**, 557–571, 1975.
- Roden, G. I., Oceanic subarctic fronts of the central North Pacific: Structure of and response to atmospheric forcing, *J. Phys. Oceanogr.*, **7**, 761–778, 1977.
- Roden, G. I., On the subtropical frontal zone north of Hawaii during winter, *J. Phys. Oceanogr.*, **10**, 342–362, 1980.
- Roden, G. I., Mesoscale oceanic fronts in the North Pacific, *Ann. Geophys.*, **2**, 399–410, 1984.
- Roden, G. I., Subarctic-subtropical transition zone of the North Pacific: Large-scale aspects and mesoscale structure, *NOAA Tech. Rep. NMFS 105*, 1–38, 1991.
- Roden, G. I., and A. R. Robinson, Subarctic frontal zone in the north-eastern Pacific: Mesoscale structure and synoptic description, *Harvard Open Ocean Model Rep.*, **31**, 68 pp., 1988.
- Ruddick, B., A practical indicator of the stability of the water column to double-diffusive activity, *Deep Sea Res., Part A*, **30**, 1105–1107, 1983.
- Samelson, R. M., and C. A. Paulson, Towed thermistor chain observations of fronts in the subtropical North Pacific, *J. Geophys. Res.*, **93**, 2237–2246, 1988.
- Stommel, H. M., A conjectural regulating mechanism for determining the thermohaline structure of the oceanic mixed layer, *J. Phys. Oceanogr.*, **23**, 142–148, 1993.
- Sverdrup, H. U., M. W. Johnson, and R. H. Fleming, *The Oceans*, 1087 pp., Prentice-Hall, Englewood Cliffs, N. J., 1942.
- Talley, L. D., Distribution and formation of North Pacific Intermediate Water, *J. Phys. Oceanogr.*, **23**, 517–537, 1993.
- Talley, L. D., T. M. Joyce, and R. A. deSzoeko, Transpacific sections at 47°N and 152°W: Distribution of properties, *Deep Sea Res., Part A*, **38**, 563–582, 1991.
- Teague, W. J., *CTD Profiles in the Northeast Pacific August–October 1982*, 335 pp., Ocean Meas. Program, U.S. Naval Oceanogr. Off., Stennis Space Cent., Miss., 1983.
- Tsuchiya, M., On the Pacific upper-water circulation, *J. Mar. Res.*, **40**, suppl., 777–799, 1982.
- Turner, J. S., *Buoyancy Effects in Fluids*, 367 pp., Cambridge Univ. Press, New York, 1973.
- Uda, M., Oceanography of the subarctic Pacific Ocean, *J. Fish. Res. Board Can.*, **20**, 119–179, 1963.
- Yoshida, T., Sea surface temperature fronts around the south boundary of the western North Pacific subarctic gyre, paper presented at the Nemuro Workshop on Western Subarctic Circulation '93, N. Pac. Mar. Sci. Org., Hokkaido, Japan, 1993.
- Yuan, X., and L. D. Talley, Shallow salinity minima in the North Pacific, *J. of Phys. Oceanogr.*, **22**, 1302–1316, 1992.
- Zhang, R., and K. Hanawa, Features of the water-mass front in the northwestern North Pacific, *J. Geophys. Res.*, **98**, 967–975, 1993.

L. D. Talley, Scripps Institution of Oceanography, University of California, San Diego, La Jolla, CA 92093-0230.

X. Yuan, Lamont-Doherty Earth Observatory, P. O. Box 1000, Route 9W, Palisades, NY 10964-8000. (e-mail: yuan@ldgo.columbia.edu)

(Received September 25, 1995; revised February 21, 1996; accepted March 19, 1996.)